Biologically relevant mechanism for catalytic superoxide removal by simple manganese compounds

Kevin Barnese[a,b], Edith Butler Gralla[a], Joan Selverstone Valentine[a,b,1], and Diane E. Cabelli[c,1]

[a]Department of Chemistry and Biochemistry, University of California, Los Angeles, CA 90095; [b]Department of Bioinspired Science, Ewha Womans University, 120-750 Seoul, Korea; and [c]Chemistry Department, Brookhaven National Laboratory, Upton, NY 11972

Contributed by Joan Selverstone Valentine, March 1, 2012 (sent for review October 3, 2011)

Nonenzymatic manganese was first shown to provide protection against superoxide toxicity in vivo in 1981, but the chemical mechanism responsible for this protection subsequently became controversial due to conflicting reports concerning the ability of Mn to catalyze superoxide disproportionation in vitro. In a recent communication, we reported that low concentrations of a simple Mn phosphate salt under physiologically relevant conditions will indeed catalyze superoxide disproportionation in vitro. We report now that two of the four Mn complexes that are expected to be most abundant in vivo, Mn phosphate and Mn carbonate, can catalyze superoxide disproportionation at physiologically relevant concentrations and pH, whereas Mn pyrophosphate and citrate complexes cannot. Additionally, the chemical mechanisms of these reactions have been studied in detail, and the rates of reactions of the catalytic removal of superoxide by Mn phosphate and carbonate have been modeled. Physiologically relevant concentrations of these compounds were found to be sufficient to mimic an effective concentration of enzymatic superoxide dismutase found in vivo. This mechanism provides a likely explanation as to how Mn combats superoxide stress in cellular systems.

pulse radiolysis | oxidative stress

The role of manganese in cells has been of great interest recently, led both by the characterization of the extraordinarily radiation-resistant bacterium *Deinococcus radiodurans*, which seems to owe some of its remarkable survival in high-radiation fields to high levels of cellular Mn (1) and by the demonstrated ability of Mn ions to rescue mutant yeast cells that have had their superoxide dismutases (SOD) removed (2).

Nonenzymatic Mn protection against superoxide O_2^- toxicity in vivo was first described in 1981 by Archibald and Fridovich (3) for the lactic acid bacterium *Lactobacillus plantarum*, which accumulates extremely high Mn levels, has no measurable enzymatic SOD activity, and yet grows normally in air. Similarly, *Neisseria gonorrhoeae*, which lack the SodA and SodC enzymes that are known to be important in *Neisseria meningitidis*, survive the challenge of O_2^- produced by the immune system. Mn accumulation has been implicated as protecting the virulent form *N. gonorrhoeae* from O_2^-, and a highly active catalase protects it from H_2O_2 (4).

Dramatic demonstrations of the antioxidant effects of Mn were reported in studies of yeast or bacteria that had been engineered to lack SOD enzymes. The health of these SOD-deficient strains, which show many defects and grow poorly in air, were greatly improved by supplementation of the growth medium with Mn(II) ion returning all tested phenotypes to normal levels (2, 5–7). The same degree of rescue was observed even if MnSOD, which is localized in the mitochondrial matrix, was also removed (6). Moreover, recent work by McNaughton et al. (8) has provided direct evidence in whole yeast cells that the concentrations of Mn phosphate complexes correlate with the ability of Mn to protect against superoxide-induced stress.

Mn can also play an antioxidant role in higher organisms, such as the nematode *Caenorhabditis elegans*. Deleterious effects due to mutations in the electron transport chain that cause higher-than-normal fluxes of reactive oxygen species and effects due to heat-shock stress are alleviated by $MnSO_4$ supplementation, which also leads to an increase in mean lifetime (9, 10).

Though the ability of Mn to protect against superoxide toxicity has now been convincingly documented in many different systems (1, 2, 4, 5, 7, 10), the in vivo chemical form of the Mn-based antioxidants and the chemical reactions responsible for their biological action remain unclear. Elucidating the exact chemical nature of the Mn-containing antioxidant molecules has proven to be particularly challenging due to the labile nature of the Mn(II) ion, which rapidly exchanges its ligands when moved from one environment to another, as occurs when it is isolated from cells. Another challenge has been the absence of a convenient direct assay for SOD activity, leading to reliance on indirect assays that may work well for SOD enzymes but are less effective for low molecular-weight metal ion complexes.

Earlier researchers explored possible mechanisms of the observed in vivo protective properties of Mn using indirect SOD assays (see below), which appeared to demonstrate that some simple Mn(II) complexes are efficient catalysts of superoxide disproportionation (11). Using those indirect assays, Mn(II) pyrophosphate, lactate, and higher concentrations of phosphate appeared to be particularly effective at superoxide removal (11). However, subsequent studies using more direct kinetic methods, such as pulse radiolysis, contradicted the earlier findings (12–14). Cabelli and Bielski (12, 13) and Barnese et al. (15) showed that O_2^- reacts rapidly with several Mn(II) compounds to form the intermediate species, $MnOO^+$, but there was little evidence of catalytic behavior.

To understand better the in vivo reactivity of Mn ions with superoxide, we have estimated the relative concentrations of the potential low molecular-weight ligands for Mn ions present in cells and determined, using their relative binding affinities for Mn(II) and Mn(III) ions, that carbonate, citrate, phosphate, and pyrophosphate bind most of the cellular Mn ions not bound to proteins (16, 17). We then investigated experimentally the reactivity of these major Mn-containing species with O_2^- under two very different conditions that might occur in vivo: O_2^- generated at lower concentrations at a constant flux or generated as a single, high-concentration burst. We report here that manganous carbonate and manganous phosphate, under physiologically relevant conditions of concentration and pH, are each capable of catalytically removing superoxide from solution at rates that are competitive with those of the cellular SOD enzymes, regardless of whether the superoxide is generated at a slow constant flux or in a single high-concentration burst.

Results

What are suitable ligands for catalytic removal of superoxide by Mn? Mn phosphate complexes have been found as the major dialyzable compound from lysates of cells with Mn-related SOD

Author contributions: K.B., E.B.G., J.S.V., and D.E.C. designed research; K.B. and D.E.C. performed research; D.E.C. contributed new reagents/analytic tools; K.B., E.B.G., J.S.V., and D.E.C. analyzed data; and K.B., E.B.G., J.S.V., and D.E.C. wrote the paper.

The authors declare no conflict of interest.

Freely available online through the PNAS open access option.

[1]To whom correspondence may be addressed. E-mail: jsv@chem.ucla.edu or cabelli@bnl.gov.

This article contains supporting information online at www.pnas.org/lookup/suppl/doi:10.1073/pnas.1203051109/-/DCSupplemental.

activity (16, 17). Recent work provides evidence in whole cells directly showing a $MnHPO_4$ complex; even more tantalizing is that its presence correlates with the ability of Mn to protect against superoxide-induced stress (8). Additionally, phosphate is a well-documented ligand in yeast and bacterial systems for Mn transport into cells and for Mn sequestering (18).

Citrate and carbonate share the characteristics of relatively strong binding affinity to Mn and relatively high concentrations in vivo. Carbonate is known to be a high-concentration component of human cells (~10 mM), and citrate is a ligand that is widely present in vivo. Additionally, Stadtman et al. (19) have demonstrated that Mn carbonate is a catalyst of H_2O_2 disproportionation, and O_2^- is an intermediate in that reaction, which demonstrates that an interesting chemistry occurs between O_2^- and $MnHCO_3^+$. Finally, carboxylate and phosphate motifs are the most commonly available ligands for Mn in vivo, being found in amino acids and nucleotides.

Initially we sought to investigate Mn compounds using the well-established cytochrome *c* SOD assay in which xanthine oxidase and xanthine in air are used to produce O_2^- (20). In agreement with earlier work, we found that Mn concentration in a phosphate buffer inversely correlated with rate of cytochrome *c* reduction, which appeared to indicate that Mn was a SOD. Upon further investigation, however, we found that the ratio of reduced cytochrome *c* to oxidized cytochrome *c* was correlated with the amount of Mn used in the experiment regardless of whether we started with fully reduced cytochrome *c*, fully oxidized cytochrome *c*, or a mixture of the two (Fig. S1). These results indicated that cytochrome *c* could be oxidized by a species created during the experiment that was proportional to available Mn (not H_2O_2), a complication that made this an unsuitable assay for SOD activity of low molecular-weight complexes of Mn.

Rather than study the mechanism behind the anomalous oxidation of cytochrome *c*, we used a different system that would allow us to simulate the traditional SOD assay without its interferences. We chose 5-(3-carboxymethoxyphenyl)-2-(4,5-dimethylthiazolyl)-3-(4-sulfophenyl) tetrazolium (MTS; structure in Fig. S2*A*) as the reporter ligand, which, unlike cytochrome *c*, is not reversibly oxidized. We generated O_2^- by ^{60}Co γ-irradiation of oxygenated aqueous solutions containing 0.5 M ethanol, which produces a constant flux of O_2^- (21). Upon reaction with O_2^-, MTS forms the colored monoformazan (MF; ε_{480nm} = 27,500 $M^{-1}\cdot cm^{-1}$; Scheme 1 and Fig. S2) compound in a rapid disproportionation reaction (22). MF forms at a rate proportional to the rate of O_2^- formation, unless the O_2^- is scavenged by another reactant. Thus, the MF formation rate is inversely proportional to the concentration and rate of the competing reactant with superoxide.

Experiments with Steady-State Conditions of Superoxide. With Mn(II) citrate present, MTS was not immediately reduced by O_2^- because the O_2^- reacted instead with the Mn(II), leading to the initial flat portion in Fig. 1*A*. Once all of the Mn(II) citrate was consumed, i.e., after the O_2^- to Mn(II) ratio surpassed 1:1, MTS was then reduced by O_2^- and the formation of MF was observed. The 1:1 stoichiometry of [Mn(II) citrate]:[O_2^-] demonstrates that O_2^- was not catalytically removed (Fig. S2*C* for close-up of area near y = 0 in Fig. 1*A*).

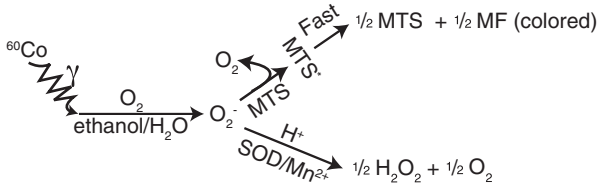

Scheme 1. Reduction of MTS by O_2^- to form MF. The reduction can be inhibited by SOD. MTS and MF structures in *SI Text*.

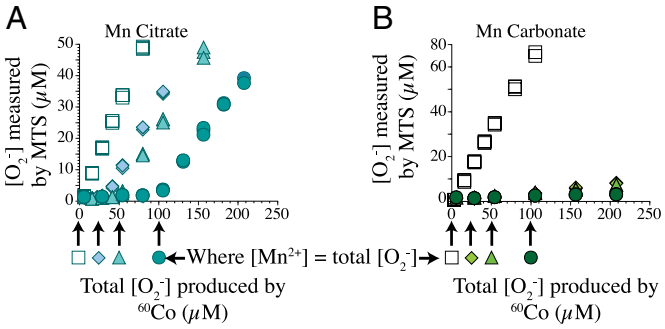

Fig. 1. $MnHCO_3^+$ catalyzes the disappearance of O_2^-, but Mn(II) citrate does not as measured by MTS reduction. O_2^- generated at 0.45 μM·s^{-1} by ^{60}Co. [O_2^-] was determined by measuring MF formation. The arrows and symbols below the *x* axis show the point of stoichiometric equivalence between O_2^- and Mn(II). Solutions contained 0, 25, 50, or 100 μM Mn, 0.5 M ethanol, 150 μM MTS, and 50 mM citrate, pH 7 (*A*), or 50 mM carbonate, pH 8 (*B*).

In contrast, $MnHCO_3^+$ [Mn(II) carbonate is noted as $MnHCO_3^+$, but in solution it may appear as $MnCO_3$; see Fig. S3 for speciation] was found to react catalytically with O_2^-. The rate of O_2^- reduction of MTS remained low, indicating that $MnHCO_3^+$ quickly removed O_2^-. The negligibly small amount of MF formed well past the point of 1:1 of [Mn(II)]:[O_2^-] indicates that the reaction was catalytic.

The data in Fig. 2*A* provide evidence as to why Mn(II) citrate reacts stoichiometrically with O_2^-. When Mn(II) citrate was reacted with O_2^-, a species that was spectroscopically similar to Mn(III) appeared at λ_{max} = 250 nm (open arrow), indicating oxidation of the Mn(II) citrate by O_2^-. Once all of the Mn(II) had been oxidized by a equal amount of O_2^-, the excess O_2^- then reacted with MTS to form the MF product at λ_{max} = 490 nm (filled arrow). The absorbance at 250–350 nm was not due to reduced MTS, because reduced MTS has much less absorbance

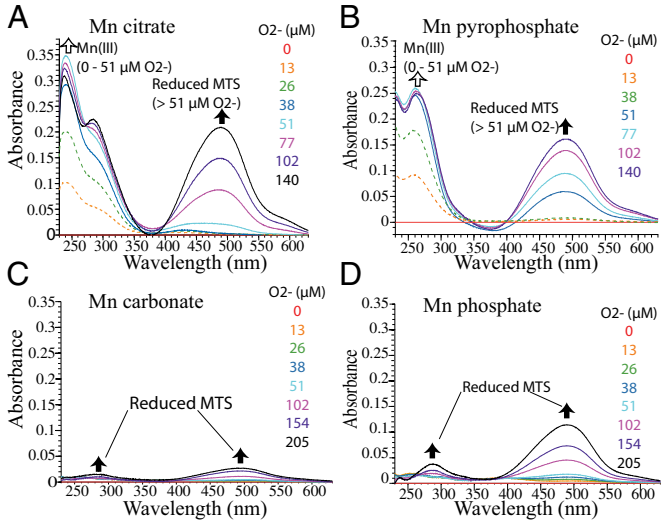

Fig. 2. $MnHCO_3^+$ and $MnHPO_4$ do not form an oxidized Mn final product when they react with O_2^- but Mn(II) citrate and $MnP_2O_7^{2-}$ do. (*A*) Mn-citrate forms a Mn(III) product (open arrow), reduction of MTS (filled arrow) occurs only after Mn(III) oxidation. (*B*) $MnHCO_3^+$ did not form a Mn(III), the reduction of MTS (filled arrow). (*C*) $MnP_2O_7^{2-}$ was similar to Mn-citrate (*A*). (*D*) $MnHPO_4$ was similar to $MnHCO_3^+$ (*B*). Solutions were irradiated with ^{60}Co to produce O_2^-. Solutions contained 50 μM MTS, 50 μM $MnSO_4$, 0.5 M ethanol, 2 U/mL catalase, and 50 mM citrate (*A*), pyrophosphate (*B*), carbonate (*C*), or phosphate (*D*). All solutions were adjusted to pH 7 except carbonate (*C*), which was pH 8.7.

in this region than at 490 nm (Fig. S2*D*). The complete oxidation of Mn(II) by O_2^- is the basis for the stoichiometric reaction.

However, when $MnHCO_3^+$ was reacted with O_2^-, a small percentage of the O_2^- reduced the MTS, and no oxidized Mn species were observed (Fig. 2*C*). These measurements were made at time points significantly longer than the lifetime of $MnOO^+$, thus there was no spectroscopic trace of the intermediate. These data indicate that $MnHCO_3^+$ catalytically cycles, because O_2^- was efficiently removed and no final stable Mn(III) product formed.

Similar experiments were performed for $MnP_2O_7^{2-}$ and $MnHPO_4$. Our previous work showed that $MnP_2O_7^{2-}$ reacted stoichiometrically with O_2^- (15). As with Mn(II) citrate, we see here $MnP_2O_7^{2-}$ becomes oxidized by one stoichiometric unit of O_2^-, as indicated by the growth of a peak at $\lambda_{max} = 260$ nm (open arrow; Fig. 2*B*). $MnHPO_4$ was shown previously to react catalytically with O_2^- (15), and in these experiments it acted similarly to $MnHCO_3^+$ (Fig. 2*D*). These data indicate that the mechanisms for $MnP_2O_7^{2-}$ and $MnHPO_4$ are similar to those for Mn(II) citrate and $MnHCO_3^+$, respectively. Comparison of the amount of MF formed in Fig. 2 *C* and *D* implies that O_2^- disappears more rapidly with $MnHCO_3^+$ than $MnHPO_4$, an observation that was further investigated by fast kinetics.

Experiments with High Initial Concentrations of Superoxide. Pulse radiolysis was used to generate bursts of O_2^-, and the changes in absorbance of any transients/final products were monitored between 225 and 375 nm as a function of time (21). This approach allowed for the direct determination of the rate constants and extinction coefficients of the intermediates. Superoxide formed within the first microsecond after the pulse (Fig. 3*A*, green triangles). The O_2^- disappeared in the presence of Mn(II) phosphate with the concomitant formation of intermediate 1 (Fig. 3*A*, purple squares). Under these conditions, this reaction occurs from 10^{-4} to 10^{-3} s. Intermediate 1 disappeared with the concomitant formation attributed to intermediate 2 (Fig. 3*A*, red circles).

The changes in absorbance with time, as measured at both 280 and 230 nm, are shown in Fig. 3 *B* and *C*, respectively. Notice that at 230 nm (Fig. 3*A*) the extinction coefficient of the first intermediate is similar to that of O_2^-, so in Fig. 3*C* the formation of the first intermediate appears as a very small change in absorbance in the first 2 ms. At 280 nm, the extinction difference between O_2^- and the first intermediate is much greater, so the rate of formation of the first intermediate is much easier to measure accurately. In contrast, the absorbance at 280 nm on the 2- to 20-ms time scale does not change much, whereas the absorbance at 230 changes significantly in the same time scale. Using these data, the absorbance changes with time for both of these processes can be fit to using pseudo-first-order kinetics. On the 50- to 500-ms time scale, the absorbances at both 230 nm and 280 nm disappear by a process that is bimolecular.

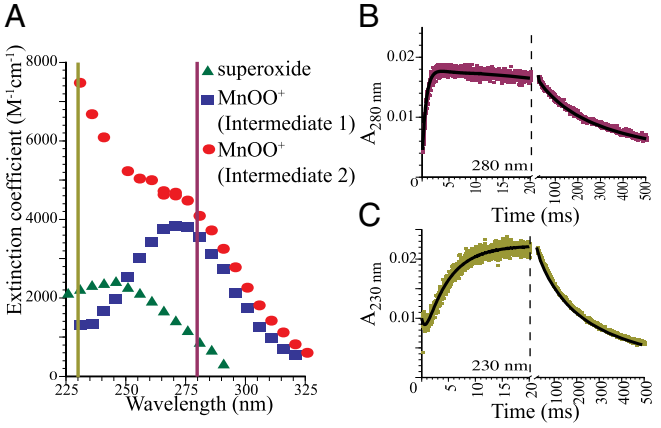

Fig. 3. Determination of rate constants and intermediate spectra by pulse radiolysis. (*A*) Spectra of different species in the reaction of O_2^- with $MnHPO_4$. The absorption bands were measured immediately after the pulse (green triangles), 2 ms after the pulse (blue squares), and 20 ms after the pulse (red circles). The pulse radiolysis trace at 280 nm (*B*) and 230 nm (*C*) were made by piecing together a 20-ms and a 500-ms time-scale trace. The solution contained 50 mM phosphate, 50 μM $MnSO_4$, 0.5 M ethanol, and ~2.4 μM O_2^- (pH 7.0).

$$Mn^{2+}\text{-}L + O_2^- \underset{k_{-1}}{\overset{k_1}{\rightleftharpoons}} MnOO^+\text{-}L \quad [1]$$

$$MnOO^+\text{-}L \xrightarrow[H^+]{k_2} Mn^{3+}\text{-}L + H_2O_2 \quad [2]$$

Scheme 2. Proposed noncatalytic mechanism of O_2^- reaction with $MnP_2O_7^{2-}$ or Mn(II) citrate. L, citrate/pyrophosphate.

For Mn(II) successfully to sequester O_2^-, a complex must be formed that does not readily dissociate. Although Mn(II) sulfate and $Mn^{2+}_{(aq)}$ react with O_2^- to readily form a $MnOO^+$ intermediate, the rate of dissociation to Mn(II) and O_2^- was sufficiently large that free O_2^- was released back into the system at low concentrations of Mn(II) (12, 23). For a Mn(II) complex to act as a SOD, the forward rate must be large with respect to the back rate. Accordingly, the reaction of Mn(II) phosphate, citrate, and carbonate complexes with O_2^- show a lack of a large intercept when a straight line is fitted through the plot of observed rates vs. [Mn] (Fig. 4), which indicates that any back reaction is minimal relative to the forward reaction.

Fast kinetic experiments show that the reaction of Mn(II) citrate with O_2^- occurs with a mechanism that is analogous to the reaction of $MnP_2O_7^{2-}$ with O_2^- (Scheme 2). At pH 7, the Mn(II) citrate reaction yielded an intermediate with a calculated rate constant for $k_1 = 1.3 \times 10^7\ M^{-1}{\cdot}s^{-1}$ and $k_{-1} < 10\ s^{-1}$. That intermediate then decayed to a final Mn(III) species with a rate of $k_2 = 2.0 \times 10^3\ s^{-1}$ (Fig. S4).

As noted above, $MnHCO_3^+$ and $MnHPO_4$ also react with a sizable forward rate and a small back rate ($MnHPO_4$ $k_3 = 2.4 \times 10^7\ M^{-1}s^{-1}$ and $k_{-3} = 10\ s^{-1}$; $MnHCO_3^+$ $k_3 = 1.4 \times 10^8\ M^{-1}{\cdot}s^{-1}$ and $k_{-3} = 7\ s^{-1}$) (Scheme 3). The successive reactions of $MnOO^+$ in phosphate or carbonate are more complicated then when citrate is the ligand, and each system is therefore discussed separately.

Reaction Kinetics of Mn(II) Phosphate with Superoxide. We found that the reaction mechanism of $MnHPO_4$ with O_2^- was dependent upon multiple factors. The rate at which Mn(II) reacts with O_2^-, k_3, was only dependent upon phosphate at phosphate concentrations <50 mM (Fig. S4). This effect is most likely due to the need for a minimum amount of phosphate to form the $MnHPO_4$ complex (8).

The observed rates for k_4, the reaction whereby a second intermediate is formed, showed a dependence on phosphate concentration (Fig. 5*A*). The rates for k_4 increased in a linear manner with increasing phosphate concentration; i.e., phosphate is fit as a first-order reactant. Phosphate concentration below 10 mM was neglected due to the small percentage of $MnHPO_4$ formed at that low phosphate concentration. We calculated the rate constant for k_4 to be $3.2 \times 10^3\ M^{-1}s^{-1}$ and k_{-4} to be $130\ s^{-1} \pm 60\ s^{-1}$.

The $MnHPO_4$ complex catalyzes superoxide removal through the disproportionation of the $MnOO^+$ complex. We studied the effects of phosphate concentration, Mn(II) concentration, and pH on k_5, the second-order rate of disappearance of the second transient. In Fig. 5*B*, we demonstrate that at higher concentrations

$$Mn^{2+}\text{-}L' + O_2^- \underset{k_{-3}}{\overset{k_3}{\rightleftharpoons}} MnOO^+\text{-}L' \quad \text{(inter 1)} \quad [3]$$

$$Anion^{n-} + MnOO^+\text{-}L' \underset{k_{-4}}{\overset{k_4}{\rightleftharpoons}} [MnOO\text{-}L'\text{-}Anion]^{n-1} \quad \text{(inter 2)} \quad [4]$$

$$MnOO^+\text{-}L' + MnOO^+\text{-}L' \xrightarrow[H^+]{k_5} 2\ Mn^{2+}\text{-}L' + H_2O_2 + O_2 \quad [5]$$

Scheme 3. Proposed catalytic mechanism of $MnHPO_4$ and $MnHCO_3^+$ disproportionation of O_2. L, phosphate/carbonate. $Anion^{n-}$ is additional bound L.

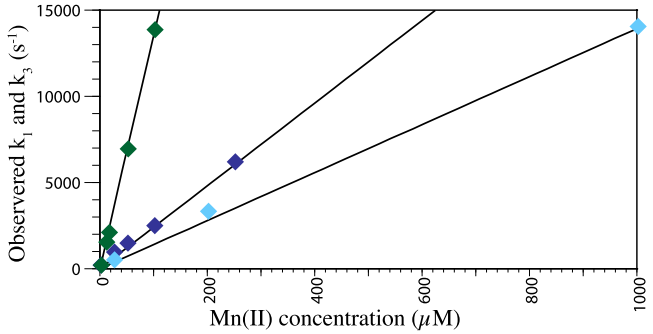

Fig. 4. The forward reaction (pseudo-first-order) of Mn(II) phosphate (blue, k_3), $MnHCO_3^+$ (green, k_3), and Mn(II) citrate (cyan, k_1) with O_2^- is fast, whereas the back reaction is slower, as determined by pulse radiolysis. Rates depend on initial [O_2^-] (1–10 μM). Solutions contained 0.5 M ethanol and 50 mM phosphate, carbonate, or citrate. All solutions were adjusted to pH 7, except carbonate, which was pH 8.7.

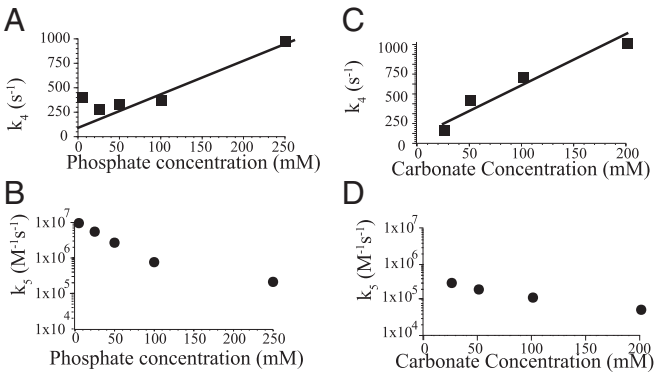

Fig. 5. Kinetics determined by pulse radiolysis. (*A* and *B*) Dependence of k_4 and k_5 on [HPO_4^{2-}]. (*C* and *D*) Dependence of k_4 and k_5 on [HCO_3^-]. Rates were fitted on initial [O_2^-] (1–10 μM). All solutions contained 0.5 M ethanol and 100 μM $MnSO_4$, and phosphate solutions were pH 7 and carbonate pH 8.3.

of phosphate there was significantly slower second-order decay. Because k_5 is bimolecular, the measured rate is more affected by concentration than a first-order reaction, and the amount of the first intermediate present in the K_4 equilibrium strongly affects the observed rate of k_5. Thus, the effect of phosphate on k_5 is likely due to shifting the equilibrium (K_4) toward a greater percentage of the second intermediate and greatly slowing k_5.

At higher pH, k_5 decreases with an apparent equilibrium point at ~pH 7.0 (Fig. S4). Speciation calculations showed that near pH 7 the dominant species is $MnHPO_4$ (Fig. S3), which may indicate that the first intermediate is more likely HPO_4MnOO^- than PO_4MnOO^{2-}. Initial Mn(II) concentration did not alter k_5 (Fig. S4) as predicted in Eq. **6** (from the rate law for Scheme 3; see *SI Text, S1* for derivation, k_{-3} neglected), because Mn(II) concentration was always higher than O_2^-. The calculated rate with only $MnOO^+$ dependence for $k_5 = 8.9 \times 10^6$ $M^{-1}{\cdot}s^{-1}$.

$$r = \frac{k_5[O_2^-]^2}{(K_4[\text{Anion}^{n-}] + 1)^2} \qquad [6]$$

Reaction Kinetics of Mn(II) Carbonate with Superoxide. The $MnHCO_3^+$ system was also studied by pulse radiolysis, and the reaction was found to be mechanistically similar to that of $MnHPO_4$ (Scheme 1), but with significantly different reaction rates. The experimental values for k_3 were relatively independent of carbonate concentration (Fig. S4), but the value of k_3 did fluctuate with changing pH (Fig. S4). Speciation calculations demonstrated that near pH 8, where the complex was studied, $MnCO_3$ and $MnHCO_3^+$ are the dominant species (Fig. S3). That the reaction rate decreases with higher pH may indicate that $MnHCO_3^+$ is a better reactant than $MnCO_3$. Also, loss of carbonate as carbon dioxide becomes a factor with lower pH.

At pH 8.3 ($MnHCO_3$), k_4 increases with increasing [HCO_3^-], analogous to the $MnHPO_4$ mechanism (Fig. 5*C*). Treating HCO_3^- as a first-order reactant, k_4 and k_{-4} were calculated to be 3.7×10^3 $M^{-1}{\cdot}s^{-1}$ and 250 $s^{-1} \pm 30$ s^{-1}, respectively. The rate of reaction 4 decreased at higher pH. This inhibition may be due to ionic effects from the increase of HCO_3^- or to the higher stability of $HOOMnHCO_3^+$ compared with $HOOMnCO_3$.

The calculated rate for $MnHCO_3^+$ k_5 (1.5×10^6 $M^{-1}{\cdot}s^{-1}$) was six-fold slower than that for $MnHPO_4$ (Fig. 5*D*). As was the case with phosphate, increased carbonate had a deleterious effect on the second-order rate of decay of the MnO_2^+ intermediate. There was also a similar trend with increasing pH. The protons either encouraged the formation of the $MnHCO_3^+$ species over the $MnCO_3$ species and/or led to an available proton to drive the formation of hydrogen peroxide from O_2^-.

Spectra of the Mn Intermediates 1 and 2. Using pulse radiolysis, intermediates generated from the reactions of O_2^- with Mn(II) citrate, $MnHPO_4$, and $MnHCO_3^+$ were found to have similar spectra (Fig. 6*A*). The λ_{max} was found near 275 nm with extinction coefficients between 4,000 and 5,000 $M^{-1}{\cdot}cm^{-1}$. The spectra are unlike the spectrum for O_2^- (λ_{max} = 245 nm and ε_{245} = 2,250 $M^{-1}{\cdot}cm^{-1}$) (24).

The spectra of the intermediates formed by reaction 4 (phosphate and carbonate) and the product formed by reaction 2 (citrate) were found to be similar to those of the respective Mn(III) complexes. Pulse radiolysis was used to generate the spectra shown in Fig. 6 *B–D* (points), and the Mn(III) complexes of the aforementioned ligands were made by various procedures and the spectra measured (lines). With $MnP_2O_7^{2-}$, this second intermediate was shown previously to be Mn(III) pyrophosphate (15). The shapes of the spectra are consistent with those of the Mn(III) ion, with a characteristic absorbance peak near 450 nm (25), indicating the species are likely in the Mn(III) oxidation state. Based on the lack of kinetic dependence of H_2O_2, intermediate 2 appears to be a Mn(III)-peroxo.

Kinetic Modeling of Rate Constants. Using Kintecus computer modeling software, we demonstrated that a physiological concentration of Mn(II) could substitute for physiological concentration of enzymatic SOD. Using rate constants determined in this work for Mn and those from Rotilio et al. (26) for yeast CuZnSOD (2×10^9 $M^{-1}{\cdot}s^{-1}$), we show that with a mere 20- to 100-fold more metal ion (Mn:Cu), Mn(II) removes O_2^- at rates similar to CuZnSOD.

Burst conditions using an initial concentration of 25 μM O_2^- (other concentrations of O_2^- showed a similar pattern) were modeled in the CuZnSOD and in the two catalytic inorganic Mn systems. To compare the different systems, the amount of O_2^- removed by the competing uncatalyzed disproportionation reaction (5.4×10^6 $M^{-1}{\cdot}s^{-1}$ at pH 7) was used as a standard, and concentrations of $MnHPO_4$ or $MnHCO_3^+$ were selected so that the amount of O_2^- lost by self-disproportionation was equal to the amount lost self-disproportionation with 1 μM CuZnSOD (Fig. 7*A*). We calculated that 1 μM of CuZnSOD is necessary for normal growth (*SI Text, S5*). Our calculations are similar to those done by Anjem et al. (27), except that they neglect to take into account that organisms can survive with much less SOD than is normally expressed (28). A concentration of 91 μM of $MnHPO_4$ or 25 μM $MnHCO_3^+$ was necessary to mimic 1 μM of CuZnSOD. The small amount of enzymatic SOD removed the O_2^- by quick catalytic cycling (Fig. 7*B*). At the chosen concentrations, Mn would quickly remove stoichiometric amounts of O_2^- to form the Mn intermediates. However, after the O_2^- is removed from the system, >99% of the Mn(II) ions would regenerate in <1.5 s.

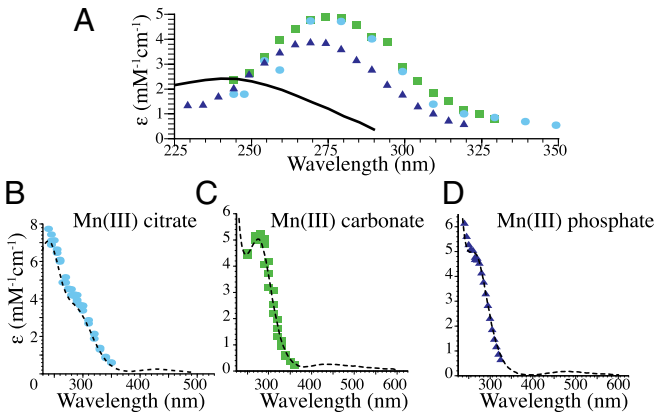

Fig. 6. Spectra of $MnOO^+$ intermediates are similar. (*A*) First intermediates and O_2^- (black line) spectra. (*B–D*) Second intermediates spectra. Pulse radiolysis was used to determine the extinction coefficient for each species at the indicated wavelengths for points in *B–D*. The dashed lines are Mn(III) samples made from Mn(III) acetate and 0.5 M carbonate or phosphate (*C* and *D*) or from ^{60}Co irradiation (*B*). Pulse radiolysis: Mn(II) citrate (circles), $MnHCO_3^+$ (squares), and $MnHPO_4$ (triangles), were made by adding 50 μM $MnSO_4$ ($MnHPO_4$ and $MnHCO_3^+$) or 200 μM $MnSO_4$ [Mn(II) citrate] to 50 mM of the corresponding anion. All solutions contained 0.5 M ethanol and were pH 7 except $MnHCO_3^+$, which was pH 7.7.

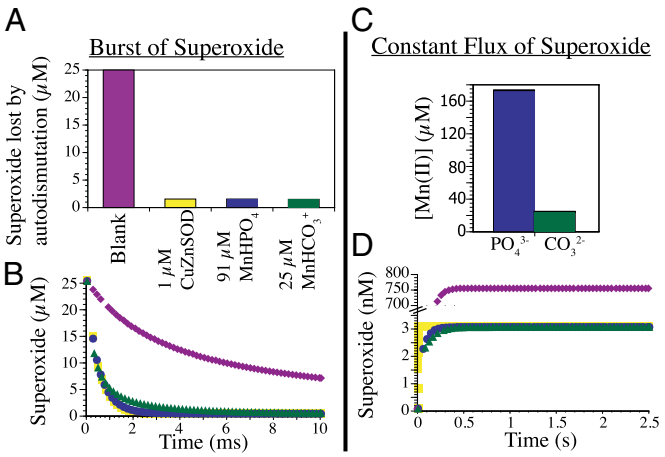

Fig. 7. Computer modeling of the catalytic superoxide dismutase activity of Mn(II) phosphate and carbonate. CuZnSOD (yellow squares) was modeled at 1 μM in all cases. The rate of autodismutation of superoxide at pH 7 was used as a competing reaction to determine noncatalytic reaction of superoxide (purple diamonds). (*A* and *B*) Superoxide was modeled as a 25-μM superoxide burst, $MnHPO_4$ (blue circles) or $MnHCO_3$ (green triangles) removed an amount of superoxide equal to that removed by 1 μM CuZnSOD. (*C* and *D*) Superoxide was modeled as a slow constant flux of 6.0 μM·s^{-1}. [Mn] with 5 mM HPO_4^{2-} or 5 mM HCO_3^- were chosen to have a steady-state $[O_2^-]$ identical to that of 1 μM CuZnSOD.

Under physiological conditions, a relatively constant O_2^- generation rate is expected. We estimated this rate at 6.0 μM/s (*SI Text, S5*). As with burst conditions, the enzymatic system cycled to remove the O_2^-, but under these conditions the Mn systems were also cycling. The rate law derived in *SI Text, S2* (which neglects k_{-3}), gives similar solutions as the computer modeling (which takes all rates into account).

The steady-state $[O_2^-]$ under conditions where O_2^- is only removed by uncatalyzed disproportionation is 750 nM (Fig. 7*D*). With 1 μM CuZnSOD, the steady-state $[O_2^-]$ was 3.0 nM. Mn concentrations were selected so that the steady-state concentration of O_2^- was also 3.0 nM; 165 μM of Mn in 5 mM phosphate or 36 μM Mn with 5 mM carbonate was necessary. The estimated value for Mn phosphate is similar to the 115 μM $MnHPO_4$ measured in yeast that was necessary to combat O_2^- stress (8), which reinforces the concept that this relatively low concentration of Mn in vivo is biologically significant.

Why is $MnHCO_3^+$ better than $MnHPO_4$ at catalytically removing O_2^- even though the rate-limiting constant for k_5 is much slower for carbonate system? The equilibrium constant for K_3 is larger with $MnHCO_3^+$ than $MnHPO_4$; therefore, the $MnHCO_3^+$ system is able to sequester the O_2^- fivefold faster than $MnHPO_4$. As a result, a higher concentration of Mn carbonate intermediate is formed than Mn phosphate intermediate from the same amount O_2^-.

Discussion

Our interest in these systems was to shed light on the observed Mn rescue of yeast and the radiation resistance that seems to be a function in part of Mn accumulation in bacterial cells. We have been able to provide a mechanism that is consistent with these phenomena and that invokes biologically relevant ligands at biologically relevant concentrations. In the process we are able to corroborate an earlier suggestion that Mn can serve as a SOD (3, 16, 29). We conclude that Archibald and Fridovich (11) were entirely correct in their conclusion that Mn(II) could catalytically remove O_2^-. However, their claim that Mn at high phosphate concentrations and $MnP_2O_7^{2-}$ could catalytically remove O_2^- were not correct because reduced cytochrome *c*, their marker of O_2^- concentrations, reacted with Mn(III) (Fig. S1).

The subsequent pulse radiolysis studies missed the catalysis by $MnHPO_4$ because the experimental conditions used in that study required the use of phosphate concentrations >250 mM due to the presence of high concentrations of the competing ligand formate, which was present in the solutions to scavenge primary radicals (13). These high concentrations of phosphate would make the intermediates appear to be stable final products on a >10-s time scale.

What gives rise to the difference between the Mn(II) phosphate and carbonate systems, which are catalytic, and the Mn(II) pyrophosphate and citrate systems, which are not? Most likely the Mn (II) citrate and pyrophosphate systems dissociate H_2O_2 (during reaction 2), but the carbonate and phosphate systems do not. Even though all of the intermediates (reactions 2 and 4) appear spectroscopically similar to Mn(III), excess hydrogen peroxide has little effect on the observed rates of the reactions. That is, free H_2O_2 does not alter observed k_4 and hence is not a reactant in k_{-4}. Additionally, speciation results (Fig. S3) show that, near pH 7, the Mn(II) citrate and $MnP_2O_7^{2-}$ complexes lack a dissociable proton, whereas the $MnHPO_4$ and $MnHCO_3^+$ do have one. The role of carbonate and phosphate may be to stabilize the superoxo/peroxo intermediate through hydrogen bonding so that H_2O_2 does not dissociate to form a Mn(III) final product.

The second-order decay has been modeled as two $MnOO^+$ intermediates interacting. This mechanism is the most likely, based on consideration of the alternatives. Another mechanism that would fit a second-order decay stems from the reaction of O_2^- with $MnOO^+$, similar to the fast reaction of O_2^- with HO_2. However, in pulse radiolysis experiments, the weak back reaction of $MnOO^+$ in carbonate or phosphate would make the concentration of O_2^- low. Additionally, one would expect that at higher Mn concentrations (less free O_2^-) this reaction would be inhibited, but we saw little dependence of Mn(II) concentration on k_5 (Fig. S4). A more likely alternative mechanism would be that the first intermediate formed reacts with the second intermediate formed. The anion concentration necessary to produce a 50/50 mixture of the first and second intermediates where the mixed reaction would be the fastest is ~50 mM (*SI Text, S4*). Our experiments do not show this trend, but experiments <50 mM may be distorted by incomplete complex formation.

We calculated that the conditions in yeast could allow Mn to serve as a defense from superoxide in vivo. However, for this inorganic Mn SOD system to be active, an organism would require concentrations of anion high enough to ensure proper

binding but low enough to inhibit the k_4 reaction. This need for tightly regulated anion concentrations makes this system unwieldy in vivo, and is a possible explanation why enzymatic SOD evolved to be nearly ubiquitous in aerobic organisms.

Currently, $MnHPO_4^+$ seems to be the best prospect as the in vivo source of SOD activity at high Mn concentrations. Although Mn carbonate remains possible, in vivo levels of carbonate can fluctuate depending on growth conditions, whereas phosphate is more tightly regulated because there are multiple enzymes dealing with import and there is a storage system. Mn carbonate also can act as a catalase (19), yet in vivo Mn has been shown not to be a catalase (27), possibly indicating that Mn is not bound to carbonate in vivo. Additionally, Daly et al. (17) have implicated Mn phosphate as the likely species protecting proteins from oxidation from radiation in *D. radiodurans*. Finally, increased in vivo Mn phosphate has been found to correlate with the ability of mutant yeast to survive superoxide stress (8).

Materials and Methods

To measure the ability of Mn(II) complexes to act as a SOD at low constant superoxide fluxes, O_2^- was generated by ^{60}Co irradiation of oxygenated 0.5 M ethanol solutions and detected by its reaction with MTS (Molecular Probes). The experiment was detailed previously (15). Briefly, ^{60}Co irradiation of samples containing 0.5 M ethanol was used to generate a flux of O_2^-. γ-Irradiation from the ^{60}Co source reacts with water, O_2, and ethanol to create superoxide at a rate of 0.45 μM/s of superoxide. MTS reacts with O_2^- to ultimately yield 1/2 monoformazan ($\varepsilon_{490\ nm}$ 27,500 $M^{-1}{\cdot}cm^{-1}$) at a rate of 2×10^5 $M^{-1}{\cdot}s^{-1}$ at pH 7 (22). In all cases, the concentration of MTS was kept sufficiently low so that the e_{aq}^- formed in the radiolysis of water reacted preferentially with O_2. Solutions buffered with different anions (phosphate, citrate, pyrophosphate, and carbonate) were oxygenated for 10 min, and then 0, 25, 50, or 100 μM Mn(II) was added. The solution was then irradiated for the time required to generate the specified amount of O_2^-. Between 5 and 10 min after the irradiation, the absorbance was read at 490 nm or the entire spectrum was recorded on a Cary UV-VIS-NIR spectrophotometer. Each time point represents the average of three separate determinations.

Pulse radiolysis experiments were carried out using a 2-MeV Van de Graff generator at Brookhaven National Laboratory. Solutions were made to the desired pH by titrating with either strong base (NaOH) or strong acid (H_2SO_4). All solutions contained 0.5 M ethanol and were bubbled with O_2 so that radicals formed by radiolysis would convert to O_2^- (21). (Carbonate solutions were oxygenated before adding concentrated carbonate buffer to inhibit loss of CO_2.) After the radiolytic pulse, O_2^- and intermediates were monitored spectrophotometrically over time (2 μs to 10 s) using a deuterium lamp (235–400 nm) and a path length of 2 cm. Because the experimental setup allows only one wavelength to be monitored at a time, spectra were determined by performing a separate experiment for each wavelength. PR software, a program designed to record and analyze the pulse radiolysis data, was used to fit data and solve for the observed rate constants and the extinction coefficients. Measurements of rate constants and spectra are within 10% error except where noted.

Solutions of Mn(III) with different ligands were made from Mn(III) acetate as follows. Both Mn(III) phosphate and carbonate were made by a modification of published protocols. Five to 10 mg of Mn(III) acetate were mixed into 5 mL of 500 mM buffer (pH 7). The slurry was syringe filtered using a 0.22-μm filter into a quartz cuvette, and the spectrum was immediately determined by a Hewlett Packard model 8452 diode array spectrophotometer. The spectrum was measured shortly after the solution was made because of the tendency for these Mn(III) complexes to disproportionate to Mn(IV) and Mn (II). The concentration of Mn(III) was calculated from extinction coefficients of the same Mn(III) species formed by pulse radiolysis (12, 13).

Mn(III) citrate was formed by oxidation of Mn(II) citrate. Oxidation was carried out using superoxide formed by ^{60}Co γ-irradiation of oxygenated 0.5 M ethanol solution. The spectrum of the Mn(III) species was then determined on a Cary UV-Vis-NIR spectrophotometer. The spectrum had the same λ_{max} as previously reported (30).

Kinetic modeling was done using Kintecus software (v3.8). Chemical equilibria were calculated using CHEAQS (http://home.tiscali.nl/cheaqs/) software and binding constants from Table S1. The equilibria were calculated taking ionic effects into account.

ACKNOWLEDGMENTS. We thank Prof. James J. Morgan of the California Institute of Technology for helpful discussions. This work was supported by National Institutes of Health Grant DK46828 (to J.S.V.). Radiolysis studies were carried out at the Accelerator Center for Energy Research at Brookhaven National Laboratory under Contract DE-AC02-98CH10886 with the US Department of Energy and supported by its Division of Chemical Sciences, Geosciences, and Biosciences, Office of Basic Energy Sciences.

1. Daly MJ, et al. (2004) Accumulation of Mn(II) in *Deinococcus radiodurans* facilitates gamma-radiation resistance. *Science* 306:1025–1028.
2. Chang EC, Kosman DJ (1989) Intracellular Mn (II)-associated superoxide scavenging activity protects Cu,Zn superoxide dismutase-deficient *Saccharomyces cerevisiae* against dioxygen stress. *J Biol Chem* 264:12172–12178.
3. Archibald FS, Fridovich I (1981) Manganese and defenses against oxygen toxicity in *Lactobacillus plantarum*. *J Bacteriol* 145:442–451.
4. Tseng HJ, Srikhanta Y, McEwan AG, Jennings MP (2001) Accumulation of manganese in *Neisseria gonorrhoeae* correlates with resistance to oxidative killing by superoxide anion and is independent of superoxide dismutase activity. *Mol Microbiol* 40: 1175–1186.
5. Al-Maghrebi M, Fridovich I, Benov L (2002) Manganese supplementation relieves the phenotypic deficits seen in superoxide-dismutase-null *Escherichia coli*. *Arch Biochem Biophys* 402:104–109.
6. Reddi AR, et al. (2009) The overlapping roles of manganese and Cu/Zn SOD in oxidative stress protection. *Free Radic Biol Med* 46:154–162.
7. Sanchez RJ, et al. (2005) Exogenous manganous ion at millimolar levels rescues all known dioxygen-sensitive phenotypes of yeast lacking CuZnSOD. *J Biol Inorg Chem* 10:913–923.
8. McNaughton RL, et al. (2010) Probing in vivo Mn2+ speciation and oxidative stress resistance in yeast cells with electron-nuclear double resonance spectroscopy. *Proc Natl Acad Sci USA* 107:15335–15339.
9. Lin YT, et al. (2006) Manganous ion supplementation accelerates wild type development, enhances stress resistance, and rescues the life span of a short-lived *Caenorhabditis elegans* mutant. *Free Radic Biol Med* 40:1185–1193.
10. Hessom JD, Srinivasan C (2007) Using elevated temperature as an assay to determine the importance of various SODs and the life extending properties of various manganese salts in *C. elegans*. *FASEB J* 21:A1040–A1040.
11. Archibald FS, Fridovich I (1982) The scavenging of superoxide radical by manganous complexes: In vitro. *Arch Biochem Biophys* 214:452–463.
12. Cabelli DE, Bielski BHJ (1984) Pulse-radiolysis study of the kinetics and mechanisms of the reactions between manganese(II) complexes and Ho2/O2- eadicals. 1. Sulfate, formate, and pyrophosphate complexes. *J Phys Chem-Us* 88:3111–3115.
13. Cabelli DE, Bielski BHJ (1984) Pulse-radiolysis study of the kinetics and mechanisms of the reactions between manganese(II) complexes and Ho2/O2- radicals. 2. The phosphate complex and an overview. *J Phys Chem-Us* 88:6291–6294.
14. Weiss RH, et al. (1993) Evaluation of activity of putative superoxide dismutase mimics. Direct analysis by stopped-flow kinetics. *J Biol Chem* 268:23049–23054.
15. Barnese K, Gralla EB, Cabelli DE, Valentine JS (2008) Manganous phosphate acts as a superoxide dismutase. *J Am Chem Soc* 130:4604–4606.
16. Archibald FS, Fridovich I (1982) Investigations of the state of the manganese in *Lactobacillus plantarum*. *Arch Biochem Biophys* 215:589–596.
17. Daly MJ, et al. (2010) Small-molecule antioxidant proteome-shields in *Deinococcus radiodurans*. *PLoS ONE* 5:e12570.
18. Reddi AR, Jensen LT, Culotta VC (2009) Manganese homeostasis in *Saccharomyces cerevisiae*. *Chem Rev* 109:4722–4732.
19. Stadtman ER, Berlett BS, Chock PB (1990) Manganese-dependent disproportionation of hydrogen peroxide in bicarbonate buffer. *Proc Natl Acad Sci USA* 87:384–388.
20. McCord JM, Fridovich I (1969) Superoxide dismutase. An enzymic function for erythrocuprein (hemocuprein). *J Biol Chem* 244:6049–6055.
21. Bielski BHJ, Gebicki JM (1982) Generation of superoxide radicals by photolysis of oxygenated ethanol solutions. *J Am Chem Soc* 104:796–798.
22. Sutherland MW, Learmonth BA (1997) The tetrazolium dyes MTS and XTT provide new quantitative assays for superoxide and superoxide dismutase. *Free Radic Res* 27: 283–289.
23. Jacobsen F, Holcman J, Sehested K (1997) Manganese(II)-superoxide complex in aqueous solution. *J Phys Chem A* 101:1324–1328.
24. Bielski BHJ, Cabelli DE, Arudi RL, Ross AB (1985) Reactivity of Ho2/O-2 radicals in aqueous-solution. *J Phys Chem Ref Data* 14:1041–1100.
25. Fackler JP, Chawla ID (1964) Spectra of manganese(III) complexes. 1. Aquomanganese (III) ion, hydroxide, fluoride, and chloride complexes. *Inorg Chem* 3:1130–1134.
26. Rotilio G, Bray RC, Fielden EM (1972) A pulse radiolysis study of superoxide dismutase. *Biochim Biophys Acta* 268:605–609.
27. Anjem A, Varghese S, Imlay JA (2009) Manganese import is a key element of the OxyR response to hydrogen peroxide in *Escherichia coli*. *Mol Microbiol* 72: 844–858.
28. Schmidt PJ, et al. (1999) Multiple protein domains contribute to the action of the copper chaperone for superoxide dismutase. *J Biol Chem* 274:23719–23725.
29. Archibald FS, Fridovich I (1981) Manganese, superoxide dismutase, and oxygen tolerance in some lactic acid bacteria. *J Bacteriol* 146:928–936.
30. Klewicki JK, Morgan JJ (1998) Kinetic behavior of Mn(III) complexes of pyrophosphate, EDTA, and citrate. *Environ Sci Technol* 32:2916–2922.